

**Nonlinear theory of solitary waves  
associated with longitudinal particle motion in lattices:  
Application to longitudinal grain oscillations  
in a dust crystal \***

I. Kourakis<sup>†</sup> and P. K. Shukla<sup>‡</sup>

*Institut für Theoretische Physik IV, Fakultät für Physik und Astronomie,  
Ruhr-Universität Bochum, D-44780 Bochum, Germany*

(Dated: submitted: 17 dec. 2003, accepted: 6 jan. 2003)

The nonlinear aspects of longitudinal motion of interacting point masses in a lattice are revisited, with emphasis on the paradigm of charged dust grains in a dusty plasma (DP) crystal. Different types of localized excitations, predicted by nonlinear wave theories, are reviewed and conditions for their occurrence (and characteristics) in DP crystals are discussed. Making use of a general formulation, allowing for an arbitrary (e.g. the Debye electrostatic or else) analytic potential form  $\phi(r)$  and arbitrarily long site-to-site range of interactions, it is shown that dust-crystals support nonlinear kink-shaped localized excitations propagating at velocities above the characteristic DP lattice sound speed  $v_0$ . Both compressive and rarefactive kink-type excitations are predicted, depending on the physical parameter values, which represent pulse- (shock-)like coherent structures for the dust grain relative displacement. Furthermore, the existence of breather-type localized oscillations, envelope-modulated wavepackets and shocks is established. The relation to previous results on atomic chains as well as to experimental results on strongly-coupled dust layers in gas discharge plasmas is discussed.

PACS numbers: 52.27.Lw, 52.35.Fp, 52.25.Vy

## I. INTRODUCTION

A wide variety of linear electrostatic waves are known to propagate in plasmas [1, 2]. It is now established that the inherent nonlinearity of electrostatic dispersive media gives birth to remarkable new phenomena, in particular related to the formation and stable propagation of long-lived nonlinear structures, when a balance between nonlinearity and dispersion is possible [3, 4]. Since about a decade ago, plasma wave theories have received a new boost after the prediction (and subsequent experimental confirmation) of the existence of new oscillatory modes, associated with charged dust-grain motion in dust-contaminated plasmas, as well as the possibility for an important modification of existing modes due to the presence of charged dust grains [5, 6]. A unique new feature associated to these dusty (or complex) plasmas (DP) is the existence of new strongly-coupled charged matter configurations, held responsible for a plethora of new phenomena e.g. phase transitions, crystallization, melting etc., and possibly even leading to the formation of dust-layers (DP crystals) when the inter-grain potential energy far exceeds the average dust

kinetic energy; a link has thus been established between plasma physics and solid state physics [7]. These dust Bravais-type quasi-lattices, which are typically formed in the sheath region in low-temperature dusty plasma discharges, and remain suspended above the negative electrode due to a balance between the electric and gravity forces [8, 9, 10, 11], are known to support harmonic excitations (acoustic modes) in both longitudinal and transverse-shear (horizontal-plane) directions, as well as optical-mode-like oscillations in the vertical (off-plane) direction [12, 13, 14, 15, 16, 17, 18, 19].

The longitudinal dust-lattice waves (LDLW) are reminiscent of waves ('phonons') propagating in atomic chains, which are long known to be dominated by nonlinear phenomena, due to the intrinsic nonlinearities of inter-atomic interaction mechanisms and/or on-site substrate potentials [20, 21, 22, 23, 24]. These phenomena have been associated with a wealth of phenomena, e.g. dislocations in crystals, energy localization, charge and information transport in bio-molecules and DNA strands, coherent signal transmission in electric lines, optical pulse propagation and many more [25, 26, 27, 28, 29]. Even though certain well-known nonlinear mechanisms, e.g. shock formation, electrostatic pulse propagation and instabilities, have been thoroughly investigated in weakly-coupled (gas-like) dusty plasmas [6, 30, 32], the theoretical investigation of the relevance of such phenomena with waves in DP crystals is still in a pre-mature stage; apart from the pioneering works of Melandsø[12], who first derived a Korteweg-DeVries (KdV) equation [31] associated with longitudinal dust-lattice oscillations, Shukla [19], who predicted the formation of dust cavitons due to lattice dynamical coupling to surrounding ions, and

---

\*Preprint; to appear in *European Physics Journal B*.

<sup>†</sup>On leave from: U.L.B. - Université Libre de Bruxelles, Physique Statistique et Plasmas C. P. 231, Boulevard du Triomphe, B-1050 Brussels, Belgium; also: Faculté des Sciences Appliquées - C.P. 165/81 Physique Générale, Avenue F. D. Roosevelt 49, B-1050 Brussels, Belgium;

Electronic address: ioannis@tp4.rub.de

<sup>‡</sup>Electronic address: ps@tp4.rub.de

the investigation of related nonlinear amplitude modulation effects by Amin *et al.* [33] a little later, not much has been done in the direction of a systematic elucidation of the relevance of dust-lattice waves being described by the known model nonlinear wave equations. It should, however, be stressed that some recent attempts to trace the signature of nonlinearity in experiments [34, 35, 36] have triggered an effort to interpret these results in terms of coherent structure propagation [35, 36, 37, 38], essentially along the physical ideas suggested in Ref. [12].

In this paper, we aim at reviewing the procedure employed in the derivation of a nonlinear evolution equation for longitudinal dust grain motion in DP lattices, and discussing the characteristics of the solutions. Emphasis is made on the methodology, in a quite exhaustive manner, in close relation with previous results on atomic chains, yet always focusing on the particular features of DP crystals; we will discuss, in particular:

- the physical assumptions underlying the continuum approximation;
- the choice of truncation scheme, when departing from the discrete lattice picture;
- the long-range electrostatic interactions, differentiating DP crystals from ordinary classical atomic chains (spring models);
- the physical relation between different solutions obtained.

Some of the results presented here are closely related to well-known previous results, yet enriched with a new analytical set of coefficients allowing for any assumed range of site-to-site interactions and any analytical form of the interaction potential. The present study is, therefore, valid in both short and long- Debye length DP cases, and also aims at providing a general ‘recipe’ which allows one, for instance, to assume a modified (possibly non-Debye-type) potential form and obtain the corresponding set of formulae in a straightforward manner. In specific, we have in mind the modification of the inter-grain interactions due to ion flow in the sheath region surrounding the dust layer, which may even lead to the crystal being destabilized, according to recent studies from first principles [39, 40].

Most of the results presented here are general and apply, in principle, to a sufficiently general class of chains of classical agents (point masses) coupled via arbitrary (and possibly long-range) interaction laws. Nevertheless, our specific aim is to establish a first link between existing nonlinear theories and the description of longitudinal dust-lattice oscillatory grain motion in a DP crystal. At a first step, our description cannot help being ‘academic’, and somewhat abstract: an ideal one-dimensional DP crystal is considered, i.e. a single, unidimensional, infinite-sized, dust-layer of identical (in size, charge and mass) dust grains situated at spatially periodic sites (at equilibrium). Effects associated with crystal asymmetries, defects, dust charging, ion-drag, dust mass variation and multiple dust-layer coupling, are left for further consideration [41]. Transverse (off-plane) mo-

tion, in particular, will be addressed in a future work.

## II. THE MODEL

### A. Equation of motion

Let us consider a layer of charged dust grains (mass  $M$ , charge  $Q$ , both assumed constant for simplicity) forming a Bravais lattice, of lattice constant  $r_0$ . The Hamiltonian of such a chain reads

$$H = \sum_n \frac{1}{2} M \left( \frac{d\mathbf{r}_n}{dt} \right)^2 + \sum_{m \neq n} U(r_{nm}),$$

where  $\mathbf{r}_n$  is the position vector of the  $n$ -th grain;  $U_{nm}(r_{nm}) \equiv Q \phi(x)$  is a binary interaction potential function related to the electrostatic potential  $\phi(x)$  around the  $m$ -th grain, and  $r_{nm} = |\mathbf{r}_n - \mathbf{r}_m|$  is the distance between the  $n$ -th and  $m$ -th grains. We shall limit ourselves to considering the *longitudinal* ( $\sim \hat{x}$ ) motion of the  $n$ -th dust grain, which obeys

$$M \left( \frac{d^2 x_n}{dt^2} + \nu \frac{dx_n}{dt} \right) = - \sum_n \frac{\partial U_{nm}(r_{nm})}{\partial x_n} \equiv Q E(x_n), \quad (1)$$

where  $E(x) = -\partial\phi(x)/\partial x$  is the electric field; the usual *ad hoc* damping term is introduced in the left-hand-side (lhs), involving the damping rate  $\nu$ , to account for the dust grain collisions with neutrals. Note that a one-dimensional (1D) DP layer is considered here, but the generalization to a two-dimensional (2D) grid is straightforward. At a first step, we have omitted the external force term  $F_{ext}$ , often introduced to account for the initial laser excitation and/or the parabolic confinement which ensures horizontal lattice equilibrium in experiments [35]. The analogous formulae for non-electrostatic, e.g. spring-like coupling interactions are readily obtained upon some trivial modifications in the notation.

The additive structure of the contribution of each site to the potential interaction force in the right-hand-side (rhs) of Eq. (1) allows us to express the electric field in (1) as:

$$\begin{aligned} E(x) &= - \frac{\partial}{\partial x_n} \sum_m \phi(x_n - x_m) \\ &= + \sum_l [\phi'(x_{n+l} - x_n) - \phi'(x_n - x_{n-l})] \\ &= \sum_{l=1}^N \sum_{l'=1}^{\infty} \frac{1}{l'!} \left. \frac{d^{l'+1} \phi(r)}{dr^{l'+1}} \right|_{r=lr_0} \times \\ &\quad [(\delta x_{n+l} - \delta x_n)^{l'} - (\delta x_n - \delta x_{n-l})^{l'}] \quad (2) \end{aligned}$$

where  $l$  denotes the degree of vicinity, i.e.  $l = 1$  accounts for the nearest-neighbour interactions (NNI) and  $l \geq 2$  accounts for distant- (second or farther) neighbour

interactions (DNI). The summation upper limit  $N$  naturally depends on the model and the interaction mechanism; even though  $N$  ‘traditionally’ equals either 1 or 2 in most studies of atomic chains, one should consider higher values for long-range-interactions e.g. Coulomb or Debye (screened) electrostatic interactions (the latter case is addressed below, in detail). In the last step, we have Taylor-developed the interaction potential  $\phi(r)$  around the equilibrium inter-grain distance  $lr_0 = |n - m|r_0$  (between  $l$ -th order neighbours), viz.

$$\phi(r_{nm}) = \sum_{l'=0}^{\infty} \frac{1}{l'!} \left. \frac{d^{l'} \phi(r)}{dr^{l'}} \right|_{r=|n-m|r_0} (x_n - x_m)^{l'},$$

where  $l'$  denotes the degree (power) of nonlinearity involved in each contribution:  $l' = 1$  is the linear interaction term,  $l' = 2$  stands for the quadratic nonlinearity, and so forth. Obviously,  $\delta x_n = x_n - x_n^{(0)}$  denotes the displacement of the  $n$ -th grain from equilibrium, which now obeys

$$\begin{aligned} M \left( \frac{d^2(\delta x_n)}{dt^2} + \nu \frac{d(\delta x_n)}{dt} \right) = & \\ & Q \left\{ \phi''(r_0) (\delta x_{n+1} + \delta x_{n-1} - 2\delta x_n) \right. \\ & + \sum_{l=2}^N \phi''(lr_0) (\delta x_{n+l} + \delta x_{n-l} - 2\delta x_n) \\ & + \sum_{l'=2}^{\infty} \frac{1}{l'!} \left. \frac{d\phi^{l'+1}(r)}{dr^{l'+1}} \right|_{r=r_0} \times \\ & \quad [(\delta x_{n+1} - \delta x_n)^{l'} - (\delta x_n - \delta x_{n-1})^{l'}] \\ & + \sum_{l=2}^N \sum_{l'=2}^{\infty} \frac{1}{l'!} \left. \frac{d\phi^{l'+1}(r)}{dr^{l'+1}} \right|_{r=lr_0} \times \\ & \quad \left. [(\delta x_{n+l} - \delta x_n)^{l'} - (\delta x_n - \delta x_{n-l})^{l'}] \right\}. \end{aligned} \quad (3)$$

We have distinguished the linear/nonlinear contributions of the first neighbors (1st/3rd lines) from the corresponding longer neighbor terms (2nd/4th lines, respectively).

Keeping all upper summation limits at infinity, the last discrete difference equation (3) is exactly equivalent to the complete equation (1). However, the former needs to be truncated to a specific order in  $l, l'$ , depending on the desired level of sophistication, for reasons of tractability.

## B. Continuum approximation.

We shall now adopt the standard continuum approximation often employed in solid state physics [7], trying to be very systematic and keeping track of any inevitable term truncation. We will assume that only small dis-

placement variations occur between neighboring sites, i.e.

$$\begin{aligned} \delta x_{n\pm l} = \delta x_n \pm lr_0 \frac{\partial u}{\partial x} + \frac{1}{2}(lr_0)^2 \frac{\partial^2 u}{\partial x^2} \\ \pm \frac{1}{3!}(lr_0)^3 \frac{\partial^3 u}{\partial x^3} + \frac{1}{4!}(lr_0)^4 \frac{\partial^4 u}{\partial x^4} + \dots, \end{aligned}$$

i.e.

$$\begin{aligned} \delta x_{n+l} - \delta x_n = lr_0 \frac{\partial u}{\partial x} + \frac{1}{2}(lr_0)^2 \frac{\partial^2 u}{\partial x^2} \\ + \frac{1}{3!}(lr_0)^3 \frac{\partial^3 u}{\partial x^3} + \frac{1}{4!}(lr_0)^4 \frac{\partial^4 u}{\partial x^4} + \dots \\ = \sum_{m=1}^{\infty} \frac{(lr_0)^m}{m!} \frac{\partial^m u}{\partial x^m}, \end{aligned} \quad (4)$$

and

$$\begin{aligned} \delta x_n - \delta x_{n-1} = lr_0 \frac{\partial u}{\partial x} - \frac{1}{2}(lr_0)^2 \frac{\partial^2 u}{\partial x^2} \\ + \frac{1}{3!}(lr_0)^3 \frac{\partial^3 u}{\partial x^3} - \frac{1}{4!}(lr_0)^4 \frac{\partial^4 u}{\partial x^4} + \dots \\ = - \sum_{m=1}^{\infty} (-1)^m \frac{(lr_0)^m}{m!} \frac{\partial^m u}{\partial x^m}, \end{aligned} \quad (5)$$

where the displacement  $\delta x(t)$  is now expressed as a continuous function  $u = u(x, t)$ .

Accordingly, the linear contributions (i.e. the first two lines) in (3) now give

$$\begin{aligned} & Q \sum_{l=1}^N \phi''(lr_0) (\delta x_{n+l} + \delta x_{n-l} - 2\delta x_n) \\ & = Q \sum_{m=1}^{\infty} \sum_{l=1}^N \phi''(lr_0) (lr_0)^{2m} \frac{2}{(2m)!} \frac{\partial^{2m} u}{\partial x^{2m}} \\ & = Q \sum_{m=1}^{\infty} \frac{2}{(2m)!} \left[ \sum_{l=1}^N \phi''(lr_0) (lr_0)^{2m} \right] \frac{\partial^{2m} u}{\partial x^{2m}} \\ & \equiv M \sum_{m=1}^{\infty} c_{2m} \frac{\partial^{2m} u}{\partial x^{2m}} \\ & = M \left( c_2 u_{xx} + c_4 u_{xxxx} + c_6 u_{xxxxxx} + \dots \right) \end{aligned} \quad (6)$$

where the subscript in  $u_x$  denotes differentiation with respect to  $x$ , i.e.  $u_{xx} = \partial^2 u / \partial x^2$  and so on. We see that only even order derivatives contribute to the linear part; this is rather expected, since the model (for  $\nu = 0$ ) is conservative, whereas odd-order derivatives might introduce a dissipative effect, e.g. via a Burgers-like ( $\sim u_{xx}$ ) additional term in the KdV Eq. below [42, 43, 44]. The definition of the coefficients  $c_{2m}$  ( $m = 1, 2, \dots$ ) is obvious; the first term reads

$$c_2 = \frac{Q}{M} r_0^2 \sum_{l=1}^N \phi''(lr_0) l^2 \equiv v_0^2 \equiv \omega_{0,L}^2 r_0^2, \quad (7)$$

which defines the characteristic second-order dispersion ('sound') velocity  $v_0$  [cf.  $v_p$  in (6) of Ref. [38]], related to the longitudinal oscillation eigenfrequency  $\omega_{0,L}$ ; also

$$c_4 = \frac{1}{12} \frac{Q}{M} r_0^4 \sum_{l=1}^N \phi''(lr_0) l^4 \equiv v_1^2 r_0^2,$$

$$c_6 = \frac{2}{6!} \frac{Q}{M} r_0^6 \sum_{l=1}^N \phi''(lr_0) l^6, \quad (8)$$

and so on. Notice that  $v_1^2 = v_0^2/12$  for NNI, i.e. if (and only if) one stops the summation at  $l_{max} = N = 1$ , like Eq. (26) in Ref. [12] [and *unlike* Eq. (5) in Ref. [38], whose 2nd term in the rhs is rather not correct, for  $l \neq 1$  i.e. DNI]. See that the 'relative weight' of any given  $2m$ -th contribution as compared to the previous one is roughly  $(2m-2)!/(2m)!$ , e.g.  $4!/6! = 1/30$  for  $m = 3$ , which somehow justifies higher (than, say,  $m = 2$ ) order contributions often neglected in the past; nevertheless, this argument should rigorously not be taken for granted, as a given function  $u(x, t)$  and/or potential  $\phi(x)$ , may present higher numerical values of higher-order derivatives, balancing this numerical effect; clearly, any truncation in an infinite series inevitably implies loss of information.

We may now treat the quadratic nonlinearity contribution in (3) (the last two lines for  $l' = 2$ ) in the same manner. Making use of Eqs. (4) and (5), and also of the identity  $a^2 - b^2 = (a+b)(a-b)$ , one obtains

$$Q \frac{1}{2!} \sum_{l=1}^N \phi'''(lr_0) \left[ (\delta x_{n+l} - \delta x_n)^2 - (\delta x_n - \delta x_{n-1})^2 \right]$$

$$= Q \sum_{m=1}^{\infty} \sum_{m'=1}^{\infty} \frac{2}{(2m-1)!(2m')!} \times$$

$$\left[ \sum_{l=1}^N \phi'''(lr_0) (lr_0)^{2(m+m')-1} \right] \frac{\partial^{2m-1} u}{\partial x^{2m-1}} \frac{\partial^{2m'} u}{\partial x^{2m'}}$$

$$\equiv M \sum_{m=1}^{\infty} \sum_{m'=1}^{\infty} c_{m,m'} \frac{\partial^{2m-1} u}{\partial x^{2m-1}} \frac{\partial^{2m'} u}{\partial x^{2m'}}$$

$$= M \left( c_{1,1} u_x u_{xx} + c_{1,2} u_x u_{xxx} \right. \\ \left. + c_{2,1} u_{xx} u_{xxx} + \dots \right). \quad (9)$$

The definition of the coefficients  $c_{m,m'}$  ( $m, m' = 1, 2, \dots$ ) is obvious; the first few terms read

$$c_{1,1} = \frac{Q}{M} r_0^3 \sum_{l=1}^N \phi'''(lr_0) l^3, \quad (10)$$

which defines the first nonlinear contribution [eg.  $B$  in Eqs. (5) and (7) in Ref. [38]; we note that a factor  $1/2$

and  $1/M$  is missing therein, respectively],

$$c_{1,2} = \frac{2}{1!4!} \frac{Q}{M} r_0^5 \sum_{l=1}^N \phi'''(lr_0) l^5,$$

$$c_{2,1} = \frac{2}{3!2!} \frac{Q}{M} r_0^5 \sum_{l=1}^N \phi'''(lr_0) l^5,$$

and so on.

The cubic nonlinearities in (3) (the last two lines for  $l' = 3$ ) may now be treated in the same manner. Making use of Eqs. (4) and (5), as well as of the identity:  $a^3 - b^3 = (a-b)(a^2 + ab + b^2)$ , one obtains

$$Q \frac{1}{3!} \sum_{l=1}^N \phi'''(lr_0) \left[ (\delta x_{n+l} - \delta x_n)^3 - (\delta x_n - \delta x_{n-1})^3 \right]$$

$$= Q \frac{1}{3} \sum_{m=1}^{\infty} \sum_{m'=1}^{\infty} \sum_{m''=1}^{\infty} \frac{1 - (-1)^{m'} + (-1)^{m'+m''}}{(2m)! m'! m''!} \times$$

$$\left[ \sum_{l=1}^N \phi'''(lr_0) (lr_0)^{2m+m'+m''} \right] \frac{\partial^{2m} u}{\partial x^{2m}} \frac{\partial^{m'} u}{\partial x^{m'}} \frac{\partial^{m''} u}{\partial x^{m''}}$$

$$\equiv M \sum_{m=1}^{\infty} c_{m,m',m''} \frac{\partial^{2m} u}{\partial x^{2m}} \frac{\partial^{m'} u}{\partial x^{m'}} \frac{\partial^{m''} u}{\partial x^{m''}}$$

$$= M \left[ c_{1,1,1} (u_x)^2 u_{xx} + (c_{1,1,2} + c_{1,2,1}) u_x (u_{xx})^2 \right. \\ \left. + c_{1,2,2} (u_{xx})^3 + \dots \right]. \quad (11)$$

The definition of the coefficients  $c_{m,m',m''}$  ( $m, m', m'' = 1, 2, \dots$ ) is obvious; their form is immediately deduced upon inspection, e.g.

$$c_{1,1,1} = \frac{1}{2} \frac{Q}{M} r_0^4 \sum_{l=1}^N \phi''''(lr_0) l^4,$$

$$c_{1,1,2} = -c_{1,2,1} = \frac{1}{12} \frac{Q}{M} r_0^5 \sum_{l=1}^N \phi''''(lr_0) l^5, \quad (12)$$

and so forth. We note that the second term in Eq. (11) cancels.

Higher order nonlinearities in Eq. (3) (the last two lines therein for  $l' \geq 4$ ), related to fifth- (or higher-) order derivatives of the interaction potential  $\phi$ , will deliberately be neglected in the following, since they are rather not likely to affect the dynamics of small grain displacements. It should be pointed out that, rigorously speaking, there is no *a priori* criterion of whether some truncation of the above infinite sums is preferable to another; some *ad hoc* truncation schemes, proposed in the past, should only be judged upon by careful numerical comparison of the

relevant contributions – e.g. in Eqs. (6), (9), (11) above – and/or, finally, a comparison of the analytical results derived to experimental ones.

Keeping the first few contributions in the above sums, one obtains the continuum analog of the discrete equation of motion

$$\ddot{u} + \nu \dot{u} - v_0^2 u_{xx} = v_1^2 r_0^2 u_{xxxx} - p_0 u_x u_{xx} + q_0 (u_x)^2 u_{xx}, \quad (13)$$

which is the final result of this section. Notice that  $u_x u_{xx} = (u_x^2)_x/2$ ; also,  $(u_x)^2 u_{xx} = (u_x^3)_x/3$ . The coefficients

$$v_0^2 \equiv c_2, \quad v_1^2 r_0^2 \equiv c_4, \quad p_0 \equiv -c_{1,1}, \quad q_0 \equiv c_{1,1,1},$$

defined by Eqs. (7), (8), (10) and (12), respectively, should be evaluated for a given potential function  $\phi$ , by truncating, if inevitable, all summations therein to a given order  $l_{max}$ . Note that, quite surprisingly, the infinite neighbour contributions may be exactly summed up, in the case of Debye (screened) electrostatic interactions, as we shall show below. Let us point out that Eq. (13) is general; the only assumption made is the continuum approximation. Also, should one prefer to improve the above truncation scheme, e.g. by including more nonlinear terms, one may readily go back to the above formulae and simply keep one or more extra term(s); in any case, one can find the exact form of all (retained and truncated) coefficients above. On the other hand, Eq. (13) generalizes the previous known results for monoatomic lattices in that it holds for an arbitrary degree of inter-site vicinity (range of interactions).

Let us point out that the above definitions of the coefficients in Eq. (13) are inspired by the Debye–Hückel (Yukawa) potential form (whose odd/even derivatives are negative/positive; see below), in which case they are defined in such a way that all of  $v_0^2$ ,  $v_1^2$ ,  $p_0$  and  $q_0$  take *positive* values. Nevertheless, keep in mind that the sign of these coefficients for a different potential function  $\phi$  is, in principle, not prescribed; indeed, analytical and numerical studies of the nature of the inter-grain interactions from first principles suggest that the presence of ion flow, for instance, may result in a structural change in the form of  $\phi$ , leading to lattice oscillation instability and presumably crystal melting [45]; see e.g. Refs. [39, 40]. However, our physical problem loses its meaning once this happens; therefore, we will assume, as a working hypothesis in the following, that  $c_2$  and  $c_4$  bear positive values (so that  $v_0$ ,  $v_1$  are real) - as a requirement for the stability of the lattice - and that, in principle (yet not necessarily), the same holds for  $p_0$  and  $q_0$ .

We observe that, upon setting  $\nu = 0$ ,  $q_0 = 0$ ,  $r_0 = a$  and  $l = 1$  (NNI), which imply that  $v_1^2 = v_0^2 a^2/12$  and  $p_0 = -Q a^3 \phi'''(a)/M \equiv \gamma(a) a^3/M$  in Eq. (13), one recovers exactly Eq. (26) in Ref. [12] [also see the definition in Eq. (16) therein]; also cf. Ref. [33]. Equations (5) – (7) in Ref. [38] are also recovered.

In the following, we will drop the damping term [second term in the right-hand-side of Eq. (13)], which is purely

phenomenological; the damping effect may then be reinserted in the analysis at any step further, by plainly adding a similar *ad hoc* term to the equation(s) modeling the grain dynamics. It may be noted that damping comes out to be weak, in experiments [35], so one may in principle proceed by including dissipation effects *a posteriori*, and then comparing theoretical or numerical results to experimental ones.

### C. An exactly computable case - the Debye ordering

Most interestingly, the summations (in  $l$ ) in the above definitions of coefficients  $c_{m,m',\dots}$  above, converge and may exactly be computed in the Debye–Hückel (Yukawa) potential case:  $\phi_D(r) = Q e^{-r/\lambda_D}/r$ , for any given number  $N$  of neighboring site vicinity:  $N = 1$  for the nearest neighbor interactions (NNI),  $N = 2$  for the second-neighbor interactions (SNI) and even  $N$  equal to infinity, for an infinite chain. The details of the calculation are given in the Appendix, so only the final result will be given here, for later use in this text. Note the definition of the *lattice parameter*  $\kappa = r_0/\lambda_D$ , to be extensively used in the following; in fact,  $\kappa$  is roughly of the order of (or slightly above) unity in laboratory experiments.

Truncating the summations at  $N = 1$  (NNI), relations (7), (8), (10) and (12) give

$$\begin{aligned} (\omega_{L,0}^{(NNI)})^2 &= \frac{2Q^2}{M\lambda_D^3} e^{-\kappa} \frac{1 + \kappa + \kappa^2/2}{\kappa^3} \\ &= (v_0^{(NNI)})^2 / (\kappa^2 \lambda_D^2) = 12(v_1^{(NNI)})^2 / (\kappa^2 \lambda_D^2), \end{aligned} \quad (14)$$

$$p_0^{(NNI)} = \frac{6Q^2}{M\lambda_D} e^{-\kappa} \left( \frac{1}{\kappa} + 1 + \frac{\kappa}{2} + \frac{\kappa^2}{6} \right), \quad (15)$$

$$q_0^{(NNI)} = \frac{12Q^2}{M\lambda_D} e^{-\kappa} \left( \frac{1}{\kappa} + 1 + \frac{\kappa}{2} + \frac{\kappa^2}{6} + \frac{\kappa^3}{24} \right). \quad (16)$$

These relations coincide with the ones in previous studies for NNI [12, 33].

Truncating the summations at  $N = 2$  (SNI), relations (7), (8), (10) and (12) give

$$\begin{aligned} (\omega_{L,0}^{(SNI)})^2 &= \frac{2Q^2}{M\lambda_D^3} \left( e^{-\kappa} \frac{1 + \kappa + \kappa^2/2}{\kappa^3} + e^{-2\kappa} \frac{\frac{1}{2} + \kappa + \kappa^2}{\kappa^3} \right) \\ &= v_0^{(SNI)2} / (\kappa^2 \lambda_D^2), \end{aligned} \quad (17)$$

accompanied by an extended set of expressions for  $v_1^{(SNI)2}$  ( $\neq (v_0^{(SNI)})^2/12$ , now, unlike in the NNI case above),  $p_0^{(SNI)}$  and  $q_0^{(SNI)}$  (see in the Appendix for details).

For higher  $l_{max} = N$ , even though the effect of adding more neighbors is cumulative, since all extra contributions are positive, these diminish fast and converge, for infinite  $N$ , to a finite set of expressions, which can be calculated via the identities:  $\sum_{l=1}^{\infty} a^l = a/(1-a)$  and  $\sum_{l=1}^{\infty} a^l/l = -\ln(1-a)$  (for  $0 < a < 1$ ); details can be found in the Appendix. This procedure is similar to the one proposed in Ref. [18] and later adopted in Refs. [35, 38]. One obtains

$$\omega_{L,0}^2 = \frac{2Q^2}{M\lambda_D^3} \frac{1}{\kappa^3} \times$$

$$\left[ e^{-\kappa/2} \frac{\kappa}{2} \operatorname{csch}\left(\frac{\kappa}{2}\right) + \frac{\kappa^2}{8} \operatorname{csch}^2\left(\frac{\kappa}{2}\right) - \ln(1 - e^{-\kappa}) \right], \quad (18)$$

for the characteristic oscillation frequency  $\omega_{L,0} = v_0/(\kappa\lambda_D)$ ; the result for  $v_0$  is obvious;  $\operatorname{csch}x = 1/\sinh x$ . A numerical investigation shows that the numerical value of the frequency in the region near  $r_0 \approx \lambda_D$  (i.e.  $\kappa \approx 1$ ) is thus increased by a factor of 1.5 or higher, roughly, compared to the NNI expression above (see Fig. 1), and so does the characteristic second-order dispersion velocity  $v_0^2 = \omega_{L,0} r_0 = \omega_{L,0} \lambda_D \kappa$  (see Fig. 2). A similar effect is witnessed for the characteristic velocity  $v_1$ , related to the fourth-order dispersion

$$v_1^2 = \frac{Q^2}{M\lambda_D} \frac{1}{96\kappa} \operatorname{csch}^4\left(\frac{\kappa}{2}\right) \times \left[ (\kappa^2 + 2) \cosh\kappa + 2(\kappa^2 - 1 + \kappa \sinh\kappa) \right] \quad (19)$$

(see Fig. 3) and for the nonlinearity coefficients

$$p_0 = \frac{Q^2}{M\lambda_D} \left\{ \frac{1}{(e^\kappa - 1)^3} \left[ 6 + e^\kappa(\kappa^2 - 3\kappa - 12) \right] + e^{2\kappa}(\kappa^2 + 3\kappa + 6) \right\} - \frac{6}{\kappa} \ln(1 + \sinh\kappa - \cosh\kappa) \quad (20)$$

and

$$q_0 = \frac{Q^2}{M\lambda_D} \left\{ \frac{1}{(e^\kappa - 1)^4} \left[ -12 + e^{2\kappa}[(\kappa^3 + 12\kappa + 48) \cosh\kappa + 2(\kappa^3 - 6\kappa - 18) + 2(\kappa^2 - 6) \sinh\kappa] \right] - \frac{12}{\kappa} \ln(1 + \sinh\kappa - \cosh\kappa) \right\}. \quad (21)$$

Upon simple inspection of Figs. 4 and 5, one deduces that  $q_0$  takes practically double the value of  $p_0$  everywhere, and thus draws the conclusion that  $q_0$  should rather *not* be omitted in Eq. (13) (cf. e.g. Refs. [12, 30, 35, 38]), for the case of the Debye potential.

### III. LINEAR OSCILLATIONS

Let us first consider the linear regime in longitudinal grain oscillations. For the sake of rigor, one may revert to the discrete formula (3) and consider its linearized form by simply neglecting the two last (double) sums therein. Inserting the ansatz  $\delta x_n \sim \exp i(nkr_0 - \omega t)$ , where  $\omega$  is the phonon frequency and  $k = 2\pi/\lambda$  (respectively,  $\lambda$ ) is the wavenumber (wavelength), one immediately obtains the general dispersion relation

$$\begin{aligned} \omega(\omega + i\nu) &= \frac{4Q}{M} \sum_{l=1}^N \phi''(lr_0) \sin^2 \frac{lkr_0}{2} \\ &= \frac{4Q}{M} \sum_{l=1}^N \phi''(l\kappa\lambda_D) \sin^2 \frac{l\kappa(k\lambda_D)}{2}. \end{aligned} \quad (22)$$

One may readily verify that the standard 1D acoustic wave dispersion relation  $\omega \approx v_0 k$  is obtained in the small  $k$  (long wavelength) limit: check by setting  $\sin(lkr_0/2) \approx lkr_0/2$  (and recalling the general definition of  $v_0$  above). Of course, taking this limit simply amounts to linearizing the continuum equation of motion derived above (and keeping the lowest contribution in  $k$ ). As pointed out before (see e.g. Ref. [18]), one thus recovers the dust-acoustic wave dispersion relation obtained in the strong-coupling dusty plasma regime (upon defining the density  $n_d$  as  $\sim r_0^{-3}$ , which may nevertheless appear somehow heuristic in this 1D model).

Notice that the form of the dispersion relation, in principle, depends on the value of  $N$ . However, in the case of the Debye interactions, i.e. explicitly substituting  $d^2\phi_D(x)/dx^2$  into (22), one obtains

$$\omega(\omega + i\nu) = \frac{4Q^2}{M\lambda_D^3} \sum_{l=1}^N e^{-l\kappa} \frac{2 + 2\kappa + (l\kappa)^2}{(l\kappa)^3} \sin^2 \frac{lkr_0}{2}. \quad (23)$$

A numerical investigation, e.g. for  $\kappa = 1$  (see Fig. 6), suggests that the dispersion curve quickly sums up to a limit curve, even for not so high values of  $N$  (practically for  $N = 2$  already). The values of the frequency reduce with increasing  $\kappa$ , as suggested by the exponential term. We see that the dispersion curve possesses a maximum at  $k = \pi/r_0 = \pi/(\kappa\lambda_D)$  for any value of  $\kappa$  and  $N$ .

The dispersion curves of dust-lattice waves have been investigated by both experiments (see e.g. Refs. [46, 47]) and *ab initio* numerical simulations [48]. It should nevertheless be acknowledged that the results of these studies do not absolutely confirm the dispersion curves obtained above, which suggests, as pointed out in Ref. [46], that one-dimensional crystal models may be inappropriate for real dust crystals.

#### IV. THE KORTEWEG – DE VRIES (KDV) EQUATION

In order to take into account weak nonlinearities, a procedure which is often adopted at a first step consists in keeping only the first nonlinear contribution in Eq. (13) (by cancelling the last term in the rhs, i.e. setting  $q_0 = 0$ ) and then considering excitations moving at a velocity close to the characteristic velocity  $v_0$ . A Galilean variable transformation, viz.

$$x \rightarrow \zeta = x - v_0 t, \quad t \rightarrow \tau = t, \quad w = u_\zeta, \quad (24)$$

then provides the KORTEWEG – DE VRIES (KdV) Equation

$$w_\tau - s a w w_\zeta + b w_{\zeta\zeta\zeta} = 0, \quad (25)$$

where a term  $u_{\tau\tau}$  was assumed of higher-order and thus neglected. The coefficients are

$$a = \frac{|p_0|}{2v_0}, \quad b = \frac{v_1^2 r_0^2}{2v_0}, \quad s = \text{sgn } p_0 = p_0/|p_0|. \quad (26)$$

We have introduced the parameter  $s$  ( $= +1/-1$ ), denoting the sign of  $p_0$ , which may change the form of the solutions (see below); as discussed above, it is equal to  $s = +1$  for the Debye-type interactions. It should be noted that this procedure is identical to the one initially adapted for dust-lattice-waves in [12] and then followed in Ref. [30, 35, 38] (for  $s = +1$ ) as may readily be checked, yet the new aspect here lies in the generalized definitions of the physical parameters above. Also notice that positive-oriented ( $\sim \hat{x}$ ) propagation was considered; adopting the above procedure in backward ( $\sim -\hat{x}$ ) propagation is trivial, yet it should be carried out by re-iterating the analytical procedure and *not* by plainly considering  $v \rightarrow -v$ : the KdV equation is *not symmetric* with respect to this transformation (also see that the velocity  $v$  appears under a square root in the formulae).

As a mathematical entity, the KdV Equation has been extensively studied [3, 27, 49, 50, 51, 52, 53, 54, 55], so only necessary details will be summarized here. It is known to possess a rich variety of solutions, including periodic (non-harmonic) solutions (cnoidal waves, involving elliptic integrals) [54]. For vanishing boundary conditions, Eq. (25) can be shown (see e.g. in Refs. [27, 55]) to possess one- or more ( $N$ -) soliton localized solutions  $w_N(\zeta, \tau)$  which bear all the well-known soliton properties: namely, they propagate at a constant profile, thanks to an exact balance between dispersive and nonlinear effects, and survive collisions between one another. The simplest (one-) soliton solution has the pulsed-shaped form

$$w_1(\zeta, \tau) = -s w_{1,m} \text{sech}^2 \left[ (\zeta - v\tau - \zeta_0)/L_0 \right], \quad (27)$$

where  $x_0$  is an arbitrary constant, denoting the initial soliton position, and  $v$  is the velocity of propagation; in

principle,  $v$  may take any real value even though its range may be physically limited, as in our case, where  $v$  has been assumed close to  $v_0$ ; this constraint will be relaxed below. A qualitative result to be retained from the soliton solution in (27) is the velocity dependence of both soliton amplitude  $w_{1,m}$  and width  $L_0$ , viz.

$$w_{1,m} = 3v/a = 6vv_0/|p_0|,$$

$$L_0 = (4b/v)^{1/2} = [2v_1^2 r_0^2 / (vv_0)]^{1/2}.$$

We see that  $w_{1,m} L_0^2 = \text{constant}$ , implying that narrower/wider solitons are taller/shorter and propagate faster/slower. These qualitative aspects of dust-lattice solitons have recently been confirmed by dust-crystal experiments [35]. Notice that the solutions of (25) satisfy an infinite set of conservation laws [3, 55]; in particular, the solitons  $w_N$  carry a constant ‘mass’  $M \sim \int w d\zeta$  (which is negative for a negative pulse), ‘momentum’  $P \sim \int w^2 d\zeta$ , ‘energy’  $P \sim \int (w_x^2/2 + u^3) d\zeta$ , and so forth (integration is understood over the entire  $x$ -axis) [52, 55]. See that the forementioned amplitude–width dependence of the 1-soliton solution (27) is heuristically deduced from the soliton ‘mass’ conservation law (implying conservation of the surface under the bell-shaped curved in Fig. 7): taller excitations have to be thinner and vice versa.

Inverting back to our initial reference frame, one obtains, for the spatial displacement variable  $u(x, t)$ , the kink/antikink (for  $s = -1/+1$ ) solitary wave form

$$u_1(x, t) = -s u_{1,m} \tanh \left[ (x - vt - x_0)/L_1 \right], \quad (28)$$

which represents a localized region of compression/rarefaction (for  $s = +1/-1$ ), propagating to the positive direction of the  $x$ -axis (see Fig. 7). The amplitude  $u_{1,m}$  and the width  $L_1$  of this shock excitation are

$$u_{1,m} = \frac{6v_1 r_0}{|p_0|} [2v_0(v - v_0)]^{1/2},$$

$$L_1 = r_0 \left[ \frac{2v_1^2}{v_0(v - v_0)} \right]^{1/2} = \frac{12v_1^2 r_0^2}{|p_0|} \frac{1}{A_m},$$

imposing ‘supersonic’ propagation ( $v > v_0$ ) for stability, in agreement with experimental results in dust crystals [35]. Notice that faster solitons will be narrower, and thus more probable to ‘feel’ the lattice discreteness, contrary to the continuum assumption above; therefore, one may impose the phenomenological criterion:  $L \ll r_0$ , amounting to the condition  $v/v_0 \gg 1 + 2v_1^2/v_0^2 \approx 1.17$  for the Debye NNI case; see (14) above], in order for the above (continuum) solution to be sustained in the (discrete) chain. Nevertheless, supersonic wave stable propagation has been numerically verified at a wide range of velocity values in atomic chains [23, 57], where Eqs. (13) and (25)

arise via a procedure similar to the one outlined above; also see Ref. [58] for a recent experiment in crystalline solids. Finally, note that  $v_0$  in real DP crystals bears values as low as a few tens of mm/sec [34, 35].

Remarkably, Eq. (25) is exactly solved via the Inverse Scattering Transform [53, 55, 56], for any given initial condition  $u(\zeta, 0)$ , which is generally seen to break-up into a number of (say  $N$ , depending on  $u(\zeta, 0)$  [56]) solitons plus a tail of background oscillations. These considerations, including, in particular, the two-soliton solution  $w_2$  of Eq. (25), which represents two distinct humps moving at different velocities and colliding during propagation without changing shape, have been postulated to be of relevance in the interpretation of recent dusty plasma discharge experiments [35, 38].

The wide reputation of the KdV Equation (25) is mostly due to the exhaustive knowledge of its analytical properties [3, 27, 51, 52, 53, 54, 55], in addition to its omni-presence in a variety of physical contexts, not excluding the physics of ordinary (ideal, i.e. electron-ion) plasmas [3, 4] and, more recently, dusty plasmas [6, 30]. However, in the above dusty-plasma-crystal context, it has been derived under specific assumptions (low discreteness and low nonlinearity effects; also, a propagation velocity  $v \approx v_0$ ) which may be questionable, in a real DP crystal. Even if the first one is virtually impossible to cope with, analytically, the latter ones may be somehow relaxed via a different approach, to be outlined below.

## V. HIGHER-ORDER KORTEWEG–DEVRIES (EKDV) EQUATIONS

In order to derive a KdV equation from the continuum equation of motion (13), we have neglected the coefficient  $q$ , which is related to the cubic nonlinearity of the interaction potential. Nevertheless, a simple numerical investigation shows that this term is *not* small, and may, in certain cases, even dominate over the quadratic term  $p$ , as in the Debye potential case (see the discussion above). Therefore, one is tempted to find out how the dynamics is modified if this term is taken into account.

### A. The Extended Korteweg – de Vries (EKdV) Equation

Repeating the procedure which led to Eq. (25), in the previous section, yet now keeping the fourth order derivative coefficient  $q \neq 0$  in Eq. (13), one obtains the EKdV Equation

$$w_\tau - s a w w_\zeta + \hat{a} w^2 w_\zeta + b w_{\zeta\zeta\zeta} = 0, \quad (29)$$

where all coefficients are given in (26) except  $\hat{a} = q_0/(2v_0)$ ; recall that  $a, b$  are positive by definition. We shall see below that  $p_0, q_0 > 0$  for Debye interactions (yet

not necessarily, in general), so that the nonlinearity coefficients, i.e.  $-sa$  (for  $s = +1$ ) and  $\hat{a}$ , bear negative and positive (respectively) values in this (Yukawa crystal) case.

The EKdV Eq. (29) was thoroughly studied in a classical series of papers by Wadati [21], who derived it for nonlinear lattices, then obtained its travelling-wave and, separately, periodic (cnoidal wave) solutions and, finally, exhaustively studied its mathematical properties. Both compressional and rarefactive solitons (say,  $w_{2,\pm}$ , to be distinguished from the KdV solution  $w_1$ ) were found to solve Eq. (29) (for either signs of  $s$ ); adapted to our notation here [59], they are of the form

$$w_2^{(1)}(\zeta, \tau) = -s v / \{ C \cosh^2[(\zeta - v\tau - \zeta_0)/L_0] + D \sinh^2[(\zeta - v\tau - \zeta_0)/L_0] \}, \quad (30)$$

and

$$w_2^{(2)}(\zeta, \tau) = +s v / \{ D \cosh^2[(\zeta - v\tau - \zeta_0)/L_0] + C \sinh^2[(\zeta - v\tau - \zeta_0)/L_0] \}, \quad (31)$$

where

$$\begin{aligned} C &= \frac{a}{6} \left( \sqrt{1 + \frac{6\hat{a}v}{a^2}} + 1 \right) \\ &= \frac{1}{12v_0} \left( \sqrt{p_0^2 + 12q_0v_0v} + |p_0| \right), \\ D &= \frac{a}{6} \left( \sqrt{1 + \frac{6\hat{a}v}{a^2}} - 1 \right) \\ &= \frac{1}{12v_0} \left( \sqrt{p_0^2 + 12q_0v_0v} - |p_0| \right), \end{aligned} \quad (32)$$

the width  $L_0$  was defined above, and  $v > 0$  is the propagation velocity. For  $s = +1/-1$ , the first expression represents a propagating localized compression/rarefaction, while the second denotes a (larger, see comment below; cf. Fig. 8) rarefaction/compression, respectively. Notice that, for  $q_0 \sim \hat{a} = 0$ , the first expression recovers the KdV result obtained previously (since  $v/C$  then recovers the KdV soliton width  $w_{1,m}$ ), while the second results in a divergent (physically unacceptable) solution [21]. Following Wadati, we may re-arrange (30) and (31) as

$$w_2^{(j)}(\zeta, \tau) = -s \epsilon_j \frac{2\sqrt{6b}}{\sqrt{\hat{a}}} \times \frac{\partial}{\partial \zeta} \left\{ \tan^{-1} \left[ \tilde{W}_2^{(j)} \tanh \left( \frac{\zeta - v\tau - \zeta_0}{L_0} \right) \right] \right\}, \quad (33)$$

provided that  $\hat{a} \sim q_0 \neq 0$ . Here

$$\tilde{W}_2^{(j)} = \left( \frac{\sqrt{1 + \frac{6\hat{a}v}{a^2}} - \epsilon_j}{\sqrt{1 + \frac{6\hat{a}v}{a^2}} + \epsilon_j} \right)^{1/2}. \quad (34)$$

Furthermore,  $v > 0$  is the propagation velocity in the frame  $\{\zeta, \tau\}$  and  $j = 1$  (2) recovers  $w_2^{(1)}$  ( $w_2^{(2)}$ ) above, so



that  $\epsilon_1$  ( $\epsilon_2$ ) is equal to  $+1$  ( $-1$ ), representing rarefactive (compressive) solutions, for  $s = +1$  – e.g. the Debye case – and vice versa for  $s = -1$  (which recovers Wadati's notation). The pulse width now depends on both  $L_0$  (defined as previously) and  $\tilde{W}_2^{(j)}$ . The pulse value for  $s = -1$  [21] satisfies:

$$w_- \equiv -(\sqrt{a^2 + 6\hat{a}v} + a) < w_2^{(1)} < 0 < w_2^{(2)} \\ < (\sqrt{a^2 + 6\hat{a}v} - a) \equiv w_+,$$

(for  $s = +1$ , one should permute the superscripts 1 and 2); since  $|w_-| > |w_+|$ , one expects, for  $s = -1$ , a small rarefactive and a large compressive pulse; the opposite holds for  $s = +1$ , e.g. in a Debye crystal case: see Fig. 8.

Inverting to the lattice displacement coordinate  $u \sim \int w d\zeta$ , expressed in the original coordinates  $\{x, t\}$ , we obtain

$$u_2^{(j)}(x, t) = -s \epsilon_j 2 \sqrt{\frac{6v_1^2}{q_0}} r_0 \times \\ \tan^{-1} \left[ W_2^{(j)} \tanh \left( \frac{x - vt - x_0}{L_1} \right) \right], \quad (35)$$

where

$$W_2^{(j)} = \left( \frac{\sqrt{p_0^2 + 12q_0 v_0 (v - v_0)} - \epsilon_j |p_0|}{\sqrt{p_0^2 + 12q_0 v_0 (v - v_0)} + \epsilon_j |p_0|} \right)^{1/2}, \quad (36)$$

and  $j = 1, 2$ . As expected, for any given  $s$  ( $= \pm 1$ ), the two different kink/antikink solutions obtained for different  $j$  ( $= 1$  or  $2$ ) are not symmetric; cf. Figure 8. Notice that the maximum value now also depends on  $W_2^{(j)}$  ( $j = 1, 2$ ).

In conclusion, the Extended KdV equation provides a more complete description of the nonlinear dynamics of the lattice, compared to the KdV equation. In particular, the EKdV compressive (rarefactive) pulse soliton obtained for  $s = +1$  ( $s = -1$ ), i.e.  $p_0 > 0$  ( $p_0 < 0$ ) is slightly smaller than its KdV counterpart (see Fig. 8), but the EKdV also predicts the possibility for a rarefactive (compressive) soliton, in either case, to form and propagate in the same lattice. In the particular case of Debye crystals, the net new result to be retained is the prediction of the existence of a rarefactive new excitation, in addition to the rarefactive one, observed in experiments. Nevertheless, theoretical studies on molecular chains seem to suggest that the additional shock-like localized mode predicted by the EKdV equation will not be as stable as its (KdV-related) counterpart. This prediction should, therefore, be confirmed numerically (and experimentally) before being taken for granted.

### B. The Modified Korteweg – de Vries (MKdV) Equation

Note, for the sake of rigor, that upon setting  $p_0 \sim a = 0$  in Eq.(29) above, one obtains a modified KdV (MKdV)

equation (with only a cubic nonlinearity term). The MKdV equation shares all the qualitative properties of the KdV Eq. and is, in fact, related to it via a Miura transformation [55]. It has two (both negative and positive, for each value of  $s$ ) pulse soliton solutions which follow immediately from the preceding solutions (30) and (31) of the EKdV equation, upon setting  $p_0 = 0$ . The remarkable additional aspect of the MKdV equation is that it also bears slowly oscillating solutions, named *breathers*, obtained just as rigorously via the inverse scattering method [22, 60]. These solutions (whose wavelength is comparable to their localized width, hence the ‘breathing’ impression and the name) share the remarkable properties of solitons; in particular, they are seen to survive collisions between themselves and with pulse solitons [22]. Their analytic form can be readily found in Refs. [22] (see §4.1 therein) and [60] and will not be reproduced here, since their condition of existence, namely  $p_0 \ll q_0$  (cf. Ref. [22]) is rather *not* satisfied in the case of Debye-interacting dust grains. Note however that breather-like excitations may exist in a DP crystal, as one may see via a different (perturbative) analysis of the nonlinear modulation of the amplitude of longitudinal lattice waves. This is considered in separate work [61].

## VI. THE BOUSSINESQ (BQ) AND GENERALIZED BOUSSINESQ (GBQ) EQUATIONS

Remember that the KdV-type equations in the preceding Section were obtained from the equation of motion (13) in an approximative manner, assuming near-sonic propagation and neglecting high-order time derivatives. Those results are therefore expected to hold for velocity values only slightly above  $v_0$ . We shall now see how these assumptions can be relaxed by directly relying on the initial (nonlinear) equation .

Let us consider Eq. (13) again (for  $\nu = 0$ ). Upon setting  $p_0 = -2p$ ,  $q_0 = 3q$ ,  $v_1^2 r_0^2 = h > 0$ , and integrating once, with respect to  $x$ , one exactly obtains, for  $w = u_x$ , the GENERALIZED BOUSSINESQ (GBq) Equation

$$\ddot{w} - v_0^2 w_{xx} = h w_{xxxx} + p (w^2)_{xx} + q (w^3)_{xx} \quad (37)$$

which, neglecting the cubic nonlinearity coefficient  $q$  [viz.  $q_0 = 0$  in (13)], reduces to the well-known Boussinesq (Bq) equation, widely studied e.g. in solid chains; see e.g. [22, 23, 57]. It possesses well-known localized solutions, whose derivation is straightforward and need not be reproduced here. The exact expressions obtained from (37) for the relative displacement  $w(x, t)$  and the longitudinal displacement  $u(x, t)$  are exhaustively presented and discussed in Refs. [22, 23]. The analytic kink/antikink-type localized solutions for  $u(x, t)$  read

$$u_3(x, t) = \mp 2 \operatorname{sgn}(h) \left( \frac{6h}{q_0} \right)^{1/2} \times$$

$$\tan^{-1} \left[ W_3 \tanh \frac{x - vt - x_0}{L_3} \right]. \quad (38)$$

Here the soliton velocity is  $v$ , while the soliton width depends on both  $W_3$  and  $L_3$ , which are

$$W_3 = \left\{ \frac{[p_0^2 + 6q_0(v^2 - v_0^2)]^{1/2} \mp |p_0|}{[p_0^2 + 6q_0(v^2 - v_0^2)]^{1/2} \pm |p_0|} \right\}^{1/2},$$

$$L_3 = 2 \left( \frac{h}{v^2 - v_0^2} \right)^{1/2}. \quad (39)$$

Recall that, for Debye interactions,  $h, q > 0$  and  $p = -p_0 < 0$  (see above), prescribing the ‘supersonic’ ( $v > v_0$ ) propagation of the solutions; the same was true of the KdV solitons obtained above. Notice, however, that the expressions obtained here for the longitudinal displacement  $u$  represent both rarefactive and compressive lattice excitations even for  $p_0 > 0$  (see Table I in [23], for  $p = -p_0 < 0$ ); remember that this feature was absent in the KdV equation (25), where  $p_0 > 0$  i.e.  $s = +1$  always led to a compressive solution in (28). In fact, this is also true of the Bq equation, which is obtained for  $q_0 = 0$ , i.e. neglecting the last term in the continuum equation of motion (13). The exact solution then reads

$$u_{Bq}(x, t) = -\text{sgn}(h) \text{sgn}(p_0) \frac{6[h(v^2 - v_0^2)]^{1/2}}{|p_0|} \times \tanh \frac{x - vt - x_0}{L_1}, \quad (40)$$

which, for positive  $h$  and  $p_0$ , prescribes only compressive supersonic kinks, pretty much like the solution  $u_1$  derived from the KdV theory above (cf. Table I in [23], for  $h_0 > 0$ ,  $p < 0$  and  $q = 0$ ).

Closing this section, one may wish to compare the GBq and Bq solutions (38) and (40), to the homologous EKdV- and KdV-related solutions (35) and (28), respectively, obtained previously: one may readily check that the former ones tend to the latter two as  $v$  tends to  $v_0$  [to see this, one may set  $v^2 - v_0^2 = (v + v_0)(v - v_0) \approx 2v_0(v^2 - v_0)$ ; recall that  $h = v_1^2 r_0^2$ ]. Nevertheless, this velocity range restriction is relaxed in the Boussinesq-related description.

## VII. EXCITATIONS IN REAL DP CRYSTALS

It is now quite tempting to observe and compare the predictions furnished by the above nonlinear models in a DP crystal in terms of excitation features, e.g. dimensions and form. For instance, one may substitute the expressions for the model’s physical parameters (i.e.  $\omega_0$ ,  $v_0$ ,  $v_1$ ,  $p_0$  and  $q_0$ ) derived in §II C into the definitions in the latter three sections, in order to derive a final form for localized excitations in a real DP crystal, in terms of the propagation velocity  $v$ , the lattice parameter  $\kappa$  and, generally, the sign  $s$  ( $= +1$  for Debye interactions). The interest in this procedure is evident, since one may seek

feedback (e.g. parameter values, excitation behaviour) from experiments and then investigate the validity of the above models by adjusting them to real DP crystal values.

The final expressions for  $u_j(x, t)$  [ $j = 1, 2, 3$ , cf. (28), (35) and (38), respectively] are somewhat lengthy and need not be reported here (since they are straightforward to derive). We may nevertheless summarize some interesting numerical results.

The soliton width  $L_1$ , as defined in (28), now becomes  $L_1 = v_0^2/p_0 u_{1,m}$ : we see that the product of the displacement  $u$  kink’s width and maximum value remains constant (regulated by the cubic interaction potential non-linearity), viz.  $u_{1,m} L_1 = 1/p_0$ , unlike the KdV pulse soliton for the relative displacement  $w = u_x$  which is characterized by  $w_{1,m} L_1^2 = cst..$  Both the kink maximum value  $u_{1,m}$  and width  $L_1$  depend on the velocity  $v$ ; as a matter of fact, faster kink excitations will be taller and narrower - see Fig. 9 - since now

$$\frac{u_{1,m}}{r_0} = \frac{v_0^2 \sqrt{6}}{p_0} \sqrt{M - 1}, \quad \frac{L_1}{r_0} = \frac{1}{\sqrt{6(M - 1)}}. \quad (41)$$

Recall that the Mach number  $M = v/v_0$  is always larger than unity. Furthermore, the magnitude of the excitation seems to decrease with  $\kappa$ ; see Fig.9a: nevertheless, very high values (near  $u/r_0 = 1$ ) observed for low  $\kappa$  and high  $v$  are rather not to be trusted, since they contradict the continuum approximation  $u \ll r_0$ .

Finally, one may compare the solutions obtained from the above theories, for a typical value of  $\kappa$ , say 1.25, according with real experimental values. The KdV-, EKdV- and Boussinesq-related kink excitations, i.e.  $u_1$ ,  $u_2$  and  $u_3$ , are depicted in Figs. 10 – 12, for three different values of  $M$ , 1.1, 1.25 and 2. We see that the EKdV and Bq models allow for both compressive and rarefactive structures, while the KdV description predicts a localized compression, which is quite sensitive to velocity changes. As expected (cf. the discussion above), both the EKdV- and Bq-related compressive excitations are similar in magnitude to the KdV-related anti-kink for near-sonic velocity (i.e. near  $M \approx 1$ ). Nevertheless, we see that the KdV-related antikink becomes taller and narrower as velocity increases, and substantially differentiates itself from its EKdV- and Bq-analogues. One may wonder whether or not the KdV picture (more familiar since widely studied) is adequate for the modeling of a real DP crystal, and also whether the rarefactive excitations predicted by other theories can indeed be sustained in the crystal. These questions may be answered by appropriate experiments and, possibly, also be investigated by numerical simulations. From a purely theoretical point of view, the Boussinesq-based description appears to be more rigorous (recall that the KdV was derived in some approximation) and valid in a more extended region than both the KdV and Extended-KdV theories.

### VIII. DISCRETENESS EFFECTS

The above analytical solutions have been derived in the continuum limit, i.e. for  $L \gg r_0$ , where  $L$  is the typical spatial dimension (width) of the solitary excitation. One may therefore define the discreteness parameter  $g = r_0/L$ , and require *a posteriori* that  $g \ll 1$ . From the expressions derived for the Bq equation above, one easily sees that  $g \sim (v^2 - v_0^2)^{1/2}/v_1$ , so this requirement is indeed fulfilled for propagation velocities  $v \approx v_0$ . However, for higher values of  $v$ , the (narrower) soliton will be subject to a variety of effects e.g. shape distortion, wave radiation etc., due to the intrinsic lattice discreteness. These effects have been investigated in solid state physics [62, 63] and may be considered with respect to DP crystals at a later stage. Let us briefly point out that narrow kink-shaped lattice excitations have been numerically shown to propagate with no considerable loss of energy, in a quite general monoatomic lattice model [62].

Also worth mentioning is the work of Rosenau [65] who derived an improved version of the Boussinesq equation (the I-Bq Eq.) in a quasi-continuum limit. The I-Bq equation, which bears the general structure of (37) upon replacing  $h u_{xxxx}$  therein by  $h u_{xxtt}$  (yet with different coefficient definitions), is not integrable and bears solitary wave solutions which do not collide elastically; nevertheless, it was numerically shown to be more stable than the Bq equation, and was argued to model discrete lattice dynamics more efficiently, upon comparison of theoretical predictions to exact numerical results [63]. Further examination of such effects may be carried out in dust-lattices, once our feedback from experiments has sufficiently determined the relevance of the issue in real DP crystals, i.e. typical excitation width, dynamics etc.

It should be underlined that the possibility for the existence of breather solitons, anticipated above, establishes a link between complex plasma ‘solid state’ modeling and the framework of discreteness-related localized excitations (discrete breathers [66], intrinsic localized modes [67]), which have recently received increasing interest among researchers in the nonlinear dynamics community. These localized modes, which are due to coupling anharmonicity and are stabilized by lattice discreteness, have been shown to exist in frequency regions forbidden to ordinary lattice waves and account for energy localization in highly discrete real crystals, where continuum theories fail. The relevance of this framework to dust crystals appears to be an interesting open area for investigation.

### IX. ENVELOPE EXCITATIONS AND SHOCKS – OPEN ISSUES

As a final interesting issue involved in the nonlinear dynamics of longitudinal lattice oscillations, let us mention the nonlinear modulation of the amplitude of dust-lattice waves, a well-known mechanism related to harmonic generation and, possibly, the modulational insta-

bility of waves propagating in lattices, eventually leading to modulated wave packet energy localization via the formation of envelope solitons [29]. This framework, which was recently also investigated with respect to low-frequency (dust-acoustic, dust-ion acoustic) electrostatic waves in dusty plasmas [32], has been partly analyzed, on the basis of the Melandsø [12] model in Ref. [33]. The authors relied on a truncated Boussinesq equation, in the form of (37) for  $q = 0$ , and succeeded in predicting the occurrence of modulational instability in LDL waves in DP crystals and the formation of envelope structures. Nevertheless, the nonlinearity coefficient  $q$  omitted therein seems to compete with  $p$  in (37) (notice the different signs) and is rather expected to affect significantly the wave’s stability profile. It should be stressed that these localized envelope excitations result from a physical mechanism which is intrinsically different from the one related to the small-amplitude excitations described in this paper; see the discussion in Ref. [68]. An extended study of this modulation nonlinear mechanism is in row and will be reported elsewhere, for clarity and conciseness.

As a final comment, we may speculate on the role of damping, herewith ignored, on the dynamics of dust-lattice waves. It is known that weak damping may balance nonlinearity, leading to the formation of shock wave fronts, as predicted in Refs. [30, 43] and confirmed by numerical simulations [44]. Furthermore, it was recently shown that the same mechanism may result in the formation of large-amplitude wide-shaped solitary waves, which may later break into a (gradually damped) train of solitons or a wavepacket depending on physical parameters [42]. We see that friction, yet weak, may play a predominant role in the life and death of localized excitations; this effect definitely deserves paying close attention with respect to waves propagating in dust crystals. Again, one would expect phenomenological theories followed by appropriately designed experiments to elucidate the friction mechanisms inherent in longitudinal dust-lattice wave propagation, in view of a more complete description than the one provided by the conservative model adopted here.

### X. CONCLUSIONS

This work was devoted to an investigation of the relevance of existing model nonlinear theories to the dynamics of longitudinal oscillations in anharmonic chains, with emphasis on dust-lattice excitations in (strongly-coupled) complex plasma crystals. Taking into account an arbitrary interaction potential and long-range interactions, we have rigorously shown that both compressive and rarefactive kink-shaped (shock-like) excitations may form and propagate in the lattice, depending basically on the mechanism of interaction between grains located at each site. These excitations are effectively modeled by either KdV- or Boussinesq-type equations, whose

analytic form was presented and whose qualitative and quantitative differences were discussed. In any case, the theory predicts coherent wave propagation above the lattice's 'sound' speed, in agreement with previous theoretical works and experimental observations (in both atomic and dust-lattices). It may be appropriate to mention that subsonic soliton propagation in monoatomic chains was also numerically considered and shown to be feasible in the past [62]. Let us point out that the model used here to pass from a discrete description to the continuum (long-wavelength) limit is quite generic, so possible modification via refined nonlinear equations may readily be obtained from it, for future consideration.

Furthermore, we have discussed the possibility of the formation of breather modes and envelope excitations, as a consequence of modulated wave packet instability, anticipating their link to discrete nonlinear theories of localized modes, left for future consideration; despite their analytical complexity, these models may, in principle, be of relevance in dust crystals due to the finite dimensions of the chain and its intrinsic spatial discreteness. Finally, the possible role played by dissipation mechanisms

has been briefly discussed.

The present study relies on, and aims at extending, previous theories on both anharmonic atomic chains and dusty plasma crystals. We hope to have succeeded in reviewing the former (extending them to the case of long-range electrostatic interactions) and generalizing the latter (which are still in an early stage). Hopefully, our predictions may be confirmed by appropriately set-up experiments, with the ambition of throwing some light in the relatively new and challenging field of strongly-coupled complex plasmas and dust-lattice dynamics.

### Acknowledgments

This work was supported by the European Commission (Brussels) through the Human Potential Research and Training Network via the project entitled: "Complex Plasmas: The Science of Laboratory Colloidal Plasmas and Mesospheric Charged Aerosols" (Contract No. HPRN-CT-2000-00140).

- 
- [1] N. A. Krall and A. W. Trivelpiece, *Principles of plasma physics*, McGraw - Hill (New York, 1973).
- [2] Th. Stix, *Waves in Plasmas*, American Institute of Physics (New York, 1992).
- [3] V. I. Karpman, *Nonlinear Waves in Dispersive Media* (Pergamon, New York, 1975).
- [4] L. Debnath (Ed.), *Nonlinear Waves* (Cambridge Univ. Press, Cambridge U.S.A., 1983).
- [5] F. Verheest, *Waves in Dusty Space Plasmas* (Kluwer Academic Publishers, Dordrecht, 2001).
- [6] P. K. Shukla and A. A. Mamun, *Introduction to Dusty Plasma Physics* (Institute of Physics, Bristol, 2002).
- [7] C. Kittel, *Introduction to Solid State Physics* (John Wiley and Sons, New York, 1996).
- [8] J. Chu and L. I, Phys. Rev. Lett. **72**, 4009 (1994).
- [9] Thomas *et al.*, Phys. Rev. Lett. **73**, 652 (1994).
- [10] A. Melzer, T. Trottenberg and A. Piel, Phys. Lett. A **191**, 301 (1994).
- [11] Y. Hayashi and K. Tachibara, Jpn. J. Appl. Phys. **33**, L84 (1994).
- [12] F. Melandsø, Phys. Plasmas **3**, 3890 (1996).
- [13] B. Farokhi *et al.*, Phys. Lett. A **264**, 318 (1999); *idem*, Phys. Plasmas **7**, 814 (2000).
- [14] S. V. Vladimirov, P. V. Shevchenko and N. F. Cramer, Phys. Rev. E **56**, R74 (1997).
- [15] G. Morfill *et al.*, in *Advances in Dusty Plasma Physics*, Eds. P. K. Shukla, D. A. Mendis and T. Desai (World Scientific, Singapore, 1997), p. 99; *idem*, Phys. Rev. Lett. **83**, 1598 (1999).
- [16] S. Nunomura, D. Samsonov and J. Goree, Phys. Rev. Lett. **84**, 5141 (2000).
- [17] D. Tskhakaya and P. S. Shukla, Phys. Lett. A **286**, 277 (2001).
- [18] X. Wang and A. Bhattacharjee, Phys. Plasmas **6**, 4388 (1999); X. Wang, A. Bhattacharjee and S. Hu, Phys. Rev. Lett. **86**, 2569 (2001).
- [19] P. K. Shukla, Phys. Lett. A **300**, 282 (2002).
- [20] A. Tsurui, Progr. Theor. Phys. **48**, 1196 (1972).
- [21] M. Wadati, J. Phys. Soc. Japan **38**, 673 (1975); *ibid* J. Phys. Soc. Japan **38**, 681 (1975).
- [22] N. Flytzanis, St. Pnevmatikos and M. Remoissenet, J. Phys. C: Solid State Phys. **18**, 4603 (1985).
- [23] St. Pnevmatikos, N. Flytzanis and M. Remoissenet, Phys. Rev. B **33**, 2308 (1986).
- [24] J. Wattis, J. Phys. A: Math. Gen. **29**, 8139 (1996).
- [25] A. S. Davydov, *Solitons in Molecular Systems* (Reidel Publ. - Kluwer, Dordrecht, 1985).
- [26] A. C. Newell and J. V. Moloney, *Nonlinear Optics* (Addison-Wesley Publ. Co., Redwood City Ca., 1992).
- [27] M. Remoissenet, *Waves Called Solitons* (Springer-Verlag, Berlin, 2nd Ed., 1996).
- [28] A. C. Scott and D. W. McLaughlin, Proc. IEEE **61**, 1443 (1973).
- [29] I. Daumont, T. Dauxois and M. Peyrard, Nonlinearity **10**, 617 (1997); M. Peyrard, Physica D **119**, 184 (1998).
- [30] P. K. Shukla, Phys. Plasmas **10**, 1619 (2003); P. K. Shukla and A. A. Mamun, New J. Phys., **5**, 17 (2003).
- [31] L. Stenflo, N. L. Tsintsadze and T. D. Buadze, Phys. Lett. A **135**, 37 (1989).
- [32] M. R. Amin, G. E. Morfill and P. K. Shukla, Phys. Rev. E **58**, 6517 (1998); I. Kourakis and P. K. Shukla, Phys. Plasmas **10**, 3459 (2003); I. Kourakis and P. K. Shukla, Physica Scripta **69**, in press (2004).
- [33] M. R. Amin, G. E. Morfill and P. K. Shukla, Phys. Scripta **58**, 628 (1998).
- [34] V. Nosenko, S. Nunomura and J. Goree, Phys. Rev. Lett. **88**, 215002 (2002).
- [35] D. Samsonov, A. V. Ivlev, R. A. Quinn, G. Morfill and S. Zhdanov, Phys. Rev. Lett. **88**, 095004 (2002).
- [36] S. Nunomura, S. Zhdanov, G. Morfill and J. Goree, Phys.

- Rev. E **68**, 026407 (2003).
- [37] S. K. Zhdanov, D. Samsonov and G. Morfill, Phys. Rev. E **66**, 026411 (2002).
- [38] K. Avinash, P. Zhu, V. Nosenko and J. Goree, Phys. Rev. E **68**, 046402 (2003).
- [39] A. M. Ignatov, Plasma Physics Reports **29**, 296 (2003).
- [40] I. Kourakis and P. K. Shukla, Phys. Lett. A **317**, 156 (2003).
- [41] G. Morfill, A. V. Ivlev and J. R. Jokipii, Phys. Rev. Lett. **83**, 971 (2000); A. Ivlev, U. Konopka and G. Morfill, Phys. Rev. E **62**, 2739 (2000); A. Ivlev and G. Morfill, Phys. Rev. E **63**, 016409 (2000).
- [42] R. Grimshaw, E. Pelinovsky and T. Talipova, Wave Motion **37**, 351 (2003).
- [43] P. K. Shukla and A. A. Mamun, IEEE Trans. Plasma Sci. **29**, 221 (2001); *ibid*, Physics of Plasmas **8**, 3216 (2001).
- [44] F. Melandsø and P. K. Shukla, Planet. Space. Sci. **43**, 635 (1995).
- [45] A. Ivlev, U. Konopka, G. Morfill and G. Joyce, Phys. Rev. E **68**, 026405 (2003).
- [46] A. Homann *et al.*, Phys. Lett. A **242**, 173 (1998).
- [47] S. Nunomura, J. Goree, S. Hu, X. Wang and A. Bhattacharjee, Phys. Rev. E **65**, 066402 (2002); S. Nunomura, J. Goree, S. Hu, X. Wang, A. Bhattacharjee and K. Avinash, Phys. Rev. Lett. **89**, 035001 (2002).
- [48] A. Melzer, Phys. Rev. E **67**, 16411 (2003); Y. Liu *et al.*, Phys. Rev. E **67**, 066408 (2003); K. Qiao and T. W. Hyde, J. Phys. A: Math. Gen. **36**, 6109 (2003).
- [49] G. B. Whitham, *Linear and Nonlinear Waves* (Wiley, New York, 1974).
- [50] K. Lonngren and A. Scott (Eds.), *Solitons in Action* (Academic, New York, 1978).
- [51] R. K. Dodd, J. C. Eilbeck, J. D. Gibbon and H. C. Morris, *Solitons and Nonlinear Wave Equations* (Academic Press, London, 1982).
- [52] See Chapters 8 in Ref. [25].
- [53] A. C. Newell, *Solitons in Mathematics and Physics* (SIAM Publ., Philadelphia, 1985).
- [54] R. Z. Sagdeev, D. A. Usikov and G. M. Zaslavsky, *Nonlinear Physics* (Harwood Academic Publishers, Philadelphia U.S.A., 1988); see Ch. 8 and 12, in particular.
- [55] P. G. Drazin and R. S. Johnson, *Solitons: an Introduction* (Cambridge Univ. Press, Cambridge, 1989).
- [56] M. J. Ablowitz and Harvey Segur, *Solitons and Inverse Scattering Transform* (SIAM, Philadelphia, 1981); V. Eckhaus and A. Van Harten, *The Inverse Scattering Transform and the Theory of Solitons, An Introduction* (North-Holland, New York, 1981).
- [57] St. Pnevmatikos, Thèse d'Etat, Université de Dijon (1984).
- [58] H. - Y. Hao and H. J. Maris, Phys. Rev. B **64**, 064302 (2001).
- [59] In order to see this, transform the variables in Ref. [21] as:  $u \rightarrow w$ ,  $x \rightarrow \zeta/\sqrt{b}$ ,  $t \rightarrow \tau/\sqrt{b}$ ,  $\alpha \rightarrow a/6$ ,  $\beta \rightarrow \hat{a}/6$ , and then insert a factor  $(-s)$ , since formulae therein for  $u$  correspond to  $s = -1$  and, upon  $u \rightarrow -u$ , to  $s = -1$  here.
- [60] G. L. Lamb Jr., *Elements of Soliton Theory* (Wiley, New York, 1980).
- [61] I. Kourakis and P. K. Shukla, submitted to Physics of Plasmas, 2003.
- [62] M. Peyrard, St. Pnevmatikos and N. Flytzanis, Physica D **19** (2), 268 (1986); N. Flytzanis, St. Pnevmatikos and M. Remoissenet, Physica D **26** (1-3), 311 (1987).
- [63] N. Flytzanis, St. Pnevmatikos and M. Remoissenet, J. Phys. A: Math. Gen. **22**, 783 (1989).
- [64] M. A. Collins, Chem. Phys. Lett. **77**, 342 (1981).
- [65] P. Rosenau, Phys. Lett. A **118**, 222 (1986); *ibid*, Physica D **27**, 224 (1986); *ibid*, Phys. Rev. B **36**, 5868 (1987).
- [66] Thierry Dauxois and Michel Peyrard, Phys. Rev. Lett. **70**, 3935 (1993); S. Flach, Phys. Rev. E **51**, 1503 (1995); T. Bountis *et al.*, Phys. Lett. **268**, 50 (2000); also see several papers in the volume: G. Tsironis and E. N. Economou (Eds.), *Fluctuations, Disorder and Nonlinearity*, Physica D **113**, North-Holland, Amsterdam (1998).
- [67] S.A.Kiselev, A. J. Sievers and S. Takeno, Phys. Rev. Lett. **61**, 970 (1988); S.R.Bickham and A.J.Sievers, Comm. Cond. Mat. Phys. **17**, 135 (1995).
- [68] R. Fedele, *Phys. Scripta* **65** 502 (2002); R. Fedele and H. Schamel, *Eur. Phys. J. B* **27** 313 (2002).

**APPENDIX A: COMPUTATION OF THE  
COEFFICIENTS FOR DEBYE (YUKAWA)  
INTERACTIONS**

Consider the Debye potential  $\phi_D(r) = Q e^{-r/\lambda_D}/r$ . Defining the (positive real) lattice parameter  $\kappa = r_0/\lambda_D$ , it is straightforward to evaluate the quantities

$$\phi'_D(lr_0) = -\frac{Q}{\lambda_D^2} e^{-l\kappa} \frac{1+l\kappa}{(l\kappa)^2},$$

$$\phi''_D(lr_0) = +\frac{2Q}{\lambda_D^3} e^{-l\kappa} \frac{1+l\kappa + \frac{(l\kappa)^2}{2}}{(l\kappa)^3},$$

$$\phi'''_D(lr_0) = -\frac{6Q}{\lambda_D^4} e^{-l\kappa} \frac{1+l\kappa + \frac{(l\kappa)^2}{2} + \frac{(l\kappa)^3}{6}}{(l\kappa)^4},$$

$$\phi''''_D(lr_0) = +\frac{24Q}{\lambda_D^5} e^{-l\kappa} \frac{1+l\kappa + \frac{(l\kappa)^2}{2} + \frac{(l\kappa)^3}{6} + \frac{(l\kappa)^4}{24}}{(l\kappa)^5},$$

where the prime denotes differentiation and  $l = 1, 2, 3, \dots$  is a positive integer. Now, we shall combine these expressions with Eqs. (7), (8), (10) and (12), defining  $v_0^2$ ,  $v_1^2$ ,  $p_0$  and  $q_0$ , respectively.

Let us define the general (families of) sum(s)

$$S_n(a) = \sum_{l=1}^{\infty} a^l l^n \quad \hat{S}_n^{(N)}(a) = \sum_{l=1}^N a^l l^n \quad (0 < a < 1), \quad (\text{A1})$$

(thinking of  $a = e^{-\kappa}$ , in particular); note that  $\hat{S}_n^{(N)}(a) \rightarrow S_n(a)$  for  $N \rightarrow \infty$ ; also,  $\hat{S}_n^{(1)}(a) = a$ . Making use of the well-known geometrical series properties:

$$S_0(a) = \sum_{l=1}^{\infty} a^l = \frac{a}{1-a} \quad \hat{S}_0^{(N)} = \sum_{l=1}^N a^l = \frac{a(1-a^N)}{1-a} \quad (0 < a < 1), \quad (\text{A2})$$

it is straightforward to derive  $S_n$ ,  $\hat{S}_n^{(N)}$  for  $l \geq 1$ , by differentiating with respect to  $a$ . One obtains

$$\begin{aligned} S_1(a) &= \sum_{l=1}^{\infty} a^l l = a \sum_{l=1}^{\infty} l a^{l-1} = a \sum_{l=1}^{\infty} \frac{\partial(a^l)}{\partial a} \\ &= a \frac{\partial}{\partial a} \sum_{l=1}^{\infty} a^l = a \frac{\partial S_0}{\partial a} = \frac{a}{(1-a)^2}. \end{aligned}$$

In a similar manner, iterating from

$$\partial^2(a^l)/\partial a^2 = l(l-1)a^{l-2} = a^{-2}(l^2 a^l - l a^l),$$

one finds

$$S_2(a) = \left( a^2 \frac{\partial^2}{\partial a^2} + a \frac{\partial}{\partial a} \right) S_0 = \dots = \frac{a(1+a)}{(1-a)^3};$$

then

$$\begin{aligned} S_3(a) &= \left( a^3 \frac{\partial^3}{\partial a^3} + 3a^2 \frac{\partial^2}{\partial a^2} + a \frac{\partial}{\partial a} \right) S_0 \\ &= \dots = \frac{a(a^2 + 4a + 1)}{(1-a)^4}, \end{aligned}$$

and so forth. Also note the identity

$$S_{-1}(a) = \sum_{l=1}^{\infty} \frac{a^l}{l} = -\ln(1-a) \quad (0 < a < 1). \quad (\text{A3})$$

The corresponding set of formulae may be obtained for  $\hat{S}_n^{(N)}$  in a similar manner.

Now, substituting  $a = e^{-\kappa}$  and using the derivatives of  $\phi_D$  above, one may immediately evaluate the expressions (7), (8), (10) and (12). Setting  $r_0 = \kappa\lambda_D$  everywhere, it is straightforward to show that

$$\begin{aligned} c_2 \equiv v_0^2 &\equiv \omega_{0,L}^2 r_0^2 = \frac{Q}{M} \kappa^2 \lambda_D^2 \sum_{l=1}^{\infty} l^2 \phi''(lr_0) = \dots \\ &= \frac{2Q^2}{M\lambda_D} \left[ \kappa^{-1} S_{-1}(e^{-\kappa}) + \kappa^0 S_0(e^{-\kappa}) + \frac{1}{2} \kappa^1 S_1(e^{-\kappa}) \right]. \end{aligned} \quad (\text{A4})$$

In the same manner

$$\begin{aligned} \frac{c_4}{r_0^2} \equiv v_1^2 &= \frac{Q}{12M} \kappa^2 \lambda_D^2 \sum_{l=1}^{\infty} l^4 \phi''(lr_0) = \dots \\ &= \frac{Q^2}{6M\lambda_D} \left[ \kappa^{-1} S_1(e^{-\kappa}) + \kappa^0 S_2(e^{-\kappa}) \right. \\ &\quad \left. + \frac{1}{2} \kappa^1 S_3(e^{-\kappa}) \right]. \end{aligned} \quad (\text{A5})$$

Also

$$\begin{aligned} p_0 \equiv -c_{11} &= -\frac{Q}{M} \kappa^3 \lambda_D^3 \sum_{l=1}^{\infty} l^3 \phi'''(lr_0) \\ &= \dots = \frac{6Q^2}{M\lambda_D} \times \\ &\quad \left[ \kappa^{-1} S_{-1}(e^{-\kappa}) + \kappa^0 S_0(e^{-\kappa}) \right. \\ &\quad \left. + \frac{1}{2} \kappa^1 S_1(e^{-\kappa}) + \frac{1}{6} \kappa^2 S_2(e^{-\kappa}) \right]. \end{aligned} \quad (\text{A6})$$

Finally, from (12) we have

$$\begin{aligned} q_0 \equiv c_{111} &= \frac{Q}{2M} \kappa^4 \lambda_D^4 \sum_{l=1}^{\infty} l^4 \phi''''(lr_0) = \dots \\ &= \frac{12Q^2}{M\lambda_D} \left[ \kappa^{-1} S_{-1}(e^{-\kappa}) + \kappa^0 S_0(e^{-\kappa}) \right. \\ &\quad \left. + \frac{1}{2} \kappa^1 S_1(e^{-\kappa}) + \frac{1}{6} \kappa^2 S_2(e^{-\kappa}) + \frac{1}{24} \kappa^3 S_3(e^{-\kappa}) \right]. \end{aligned} \quad (\text{A7})$$

The corresponding expressions for a value of  $N$  are given by substituting  $S_n(\cdot)$  with  $\hat{S}_n^{(N)}(\cdot)$  everywhere. One immediately sees that  $p_0/v_0^2 > 2$ ,  $q_0/v_0^2 > 6$ ; also,  $v_1^2/v_0^2 = 12$  for  $N = 1$  (only), i.e. for the NNI case.

Finally, combining the above exact expressions for  $S_{-1}(a)$ , ...,  $S_3(a)$ , we obtain exactly expressions (18) to (21) in the text.

## Figure Captions

Figure 1.

(a) The linear oscillation frequency squared  $\omega^2$  (normalized over  $Q^2/(M\lambda_D^3)$ ) is depicted against the lattice constant  $\kappa$ , for  $N = 1$  (first-neighbor interactions: —),  $N = 2$  (second-neighbor interactions: - - -),  $N = \infty$  (infinite-neighbors: - - -), from bottom to top. (b) Detail near  $\kappa \approx 1$ .

Figure 2.

(a) The characteristic 2nd order dispersion velocity squared  $v_0^2$  (normalized over  $Q^2/(M\lambda_D)$ ) is depicted against the lattice constant  $\kappa$ , for  $N = 1$  (first-neighbor interactions: —),  $N = 2$  (second-neighbor interactions: - - -),  $N = \infty$  (infinite-neighbors: - - -), from bottom to top. (b) Detail near  $\kappa \approx 1$ .

Figure 3.

(a) The characteristic 4th order dispersion velocity squared  $v_1^2$  (normalized over  $Q^2/(M\lambda_D)$ ) is depicted against the lattice constant  $\kappa$ , for  $N = 1$  (first-neighbor interactions: —),  $N = 2$  (second-neighbor interactions: - - -),  $N = \infty$  (infinite-neighbors: - - -), from bottom to top. (b) Detail near  $\kappa \approx 1$ .

Figure 4.

(a) The nonlinearity coefficient  $p_0$  (normalized over  $Q^2/(M\lambda_D)$ ) is depicted against the lattice constant  $\kappa$  for  $N = 1$  (first-neighbor interactions: —),  $N = 2$  (second-neighbor interactions: - - -),  $N = \infty$  (infinite-neighbors: - - -), from bottom to top. (b) Detail near  $\kappa \approx 1$ .

Figure 5.

(a) The nonlinearity coefficient  $q_0$  (normalized over  $Q^2/(M\lambda_D)$ ) is depicted against the lattice constant  $\kappa$  for  $N = 1$  (first-neighbor interactions: —),  $N = 2$  (second-neighbor interactions: - - -),  $N = \infty$  (infinite-neighbors: - - -), from bottom to top. (b) Detail near  $\kappa \approx 1$ .

Figure 6.

Dispersion relation for the Debye interactions, neglecting damping; cf. (23) for  $\nu = 0$ : the square frequency  $\omega^2$ , normalized over  $Q^2/(M\lambda_D^3)$ , is depicted versus the normalized wavenumber  $kr_0/\pi$  for  $N = 1$  (first-neighbor interactions: —),  $N = 2$  (second-neighbor interactions: - - -),  $N = 7$  (up to 7th nearest-neighbors: - - -), i.e. from bottom to top.

Figure 7.

Localized antikink/kink (negative/positive pulse) functions, related to the KdV Eq. (25), for the displacement  $u(x, t)$  (relative displacement  $w(x, t) \sim \partial u(x, t)/\partial x$ ), for positive/negative  $p_0$  coefficient i.e.  $s = +1/-1$ , are depicted in figures (a)/(b); recall that (a) holds for Debye interactions; arbitrary parameter values:

$v = 1$  (solid curve),  $v = 2$  (long dashed curve),  $v = 3$  (short dashed curve).

Figure 8.

(a) The two localized pulse solutions of the EKdV Eq. (29) for the relative displacement  $w(x, t) \sim \partial u(x, t)/\partial x$  are depicted for some set of (positive) values of the  $p_0$  and  $q_0$  coefficients (i.e.  $s = +1$ ): the first (dashed curve)/second (short-dashed) solution, as given by (30)/(31), represents the smaller negative/larger positive pulses. The larger negative pulse (solid curve) denotes the solution of the KdV Eq. (25) for the same parameter set. (b) The corresponding solutions for the particle displacement  $u(x, t)$ .

Figure 9.

(a) The (normalized) maximum value of the kink-shaped localized displacement  $u_1(x, t)/r_0$ , as obtained from the KdV Equation, is depicted versus the lattice parameter  $\kappa$  and the normalized velocity (Mach number)  $M = v/v_0$ . (b) The (normalized) width  $L_1/r_0$  of  $u_1(x, t)$  is depicted against  $M = v/v_0$ .

Figure 10.

The antikink excitation predicted by the KdV theory (solid curve) is compared to the (two) solutions obtained from (a) the EkDV Equation; (b) the Bq Equation-related model (dashed curves). Values: lattice parameter  $\kappa = 1.1$ , normalized velocity (Mach number)  $M = v/v_0 = 1.25$ .

Figure 11.

Similar to Fig. 10, for  $M = v/v_0 = 1.25$ .

Figure 12.

Similar to Figs. 11 and 12, for  $M = v/v_0 = 2$ .

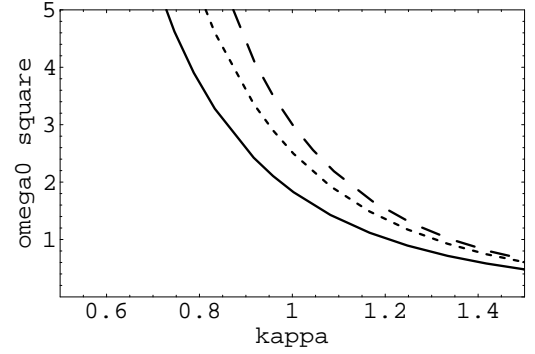
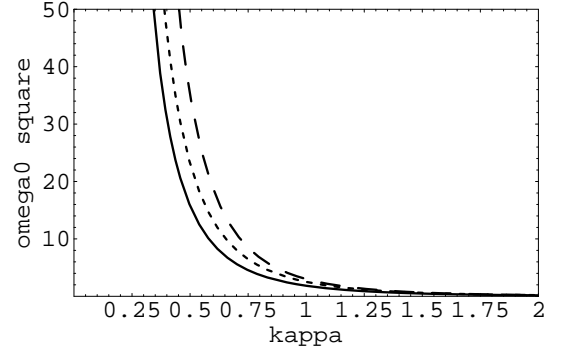


FIG. 1:



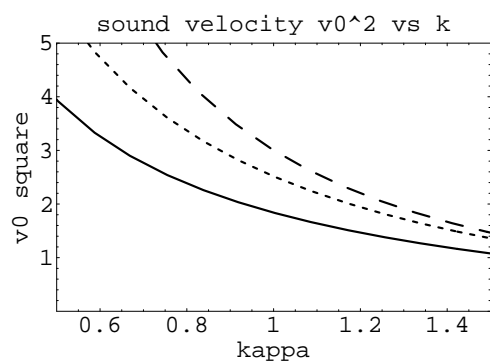
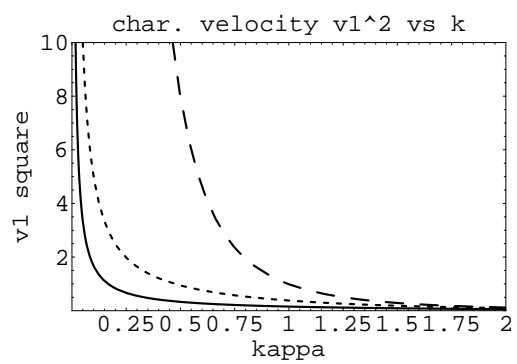
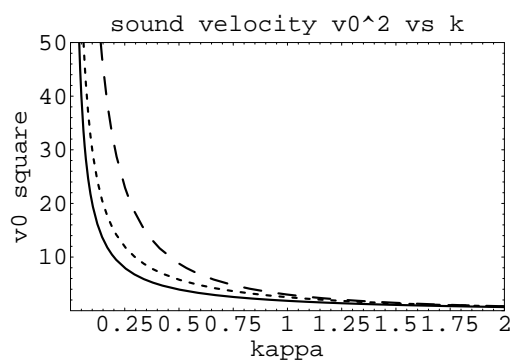


FIG. 2:

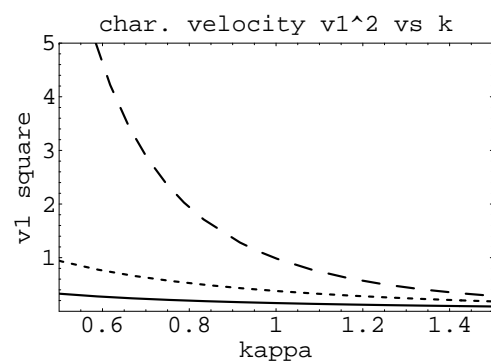


FIG. 3:

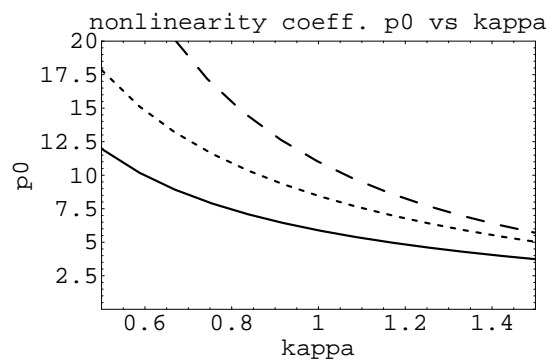
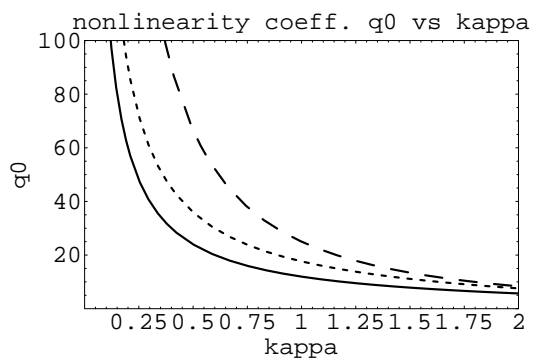
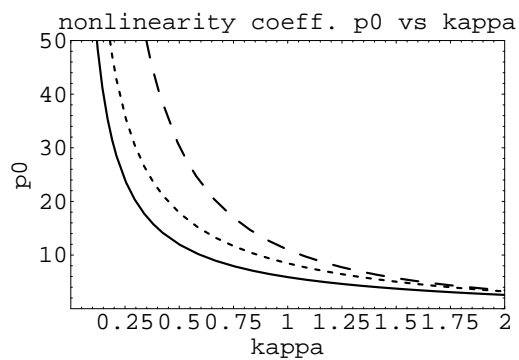


FIG. 4:

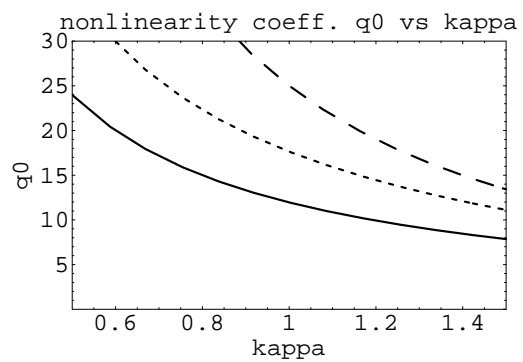


FIG. 5:

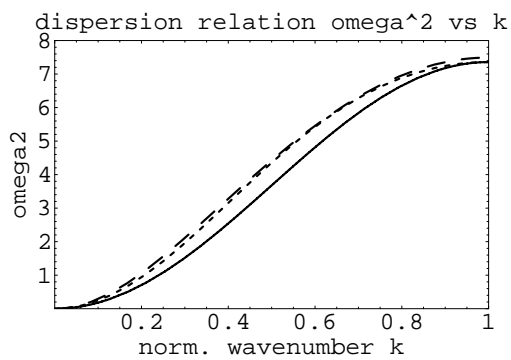


FIG. 6:

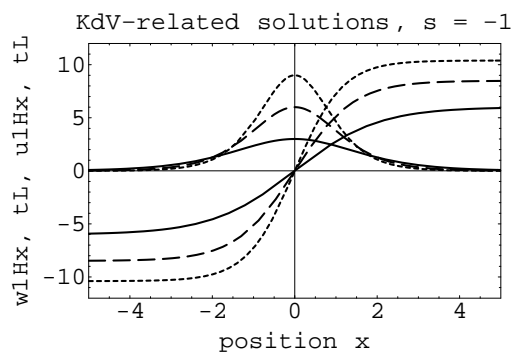
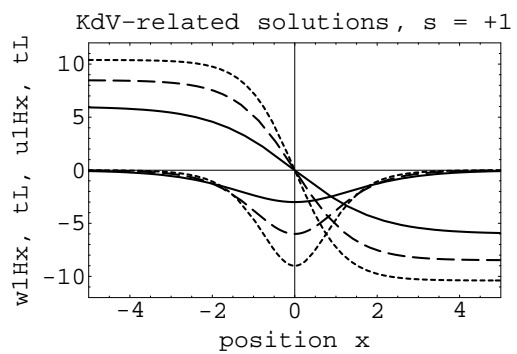


FIG. 7:

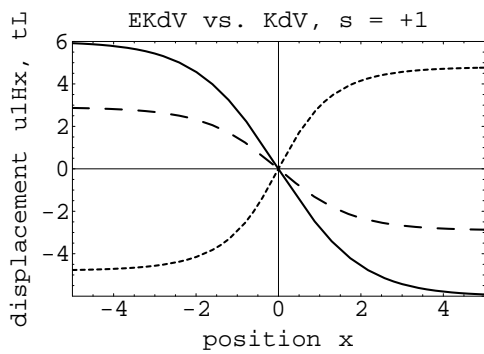
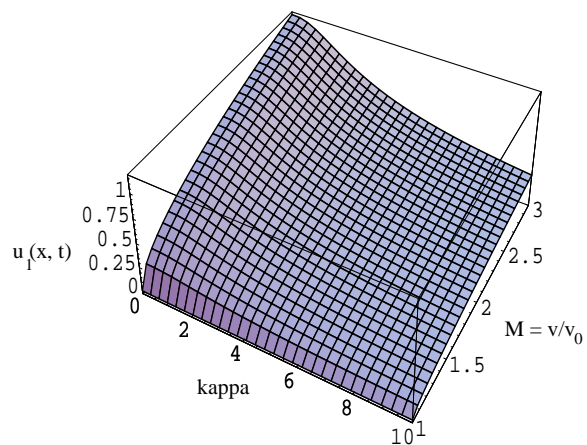
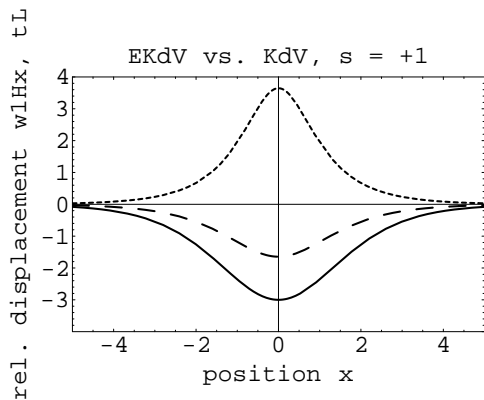


FIG. 8:

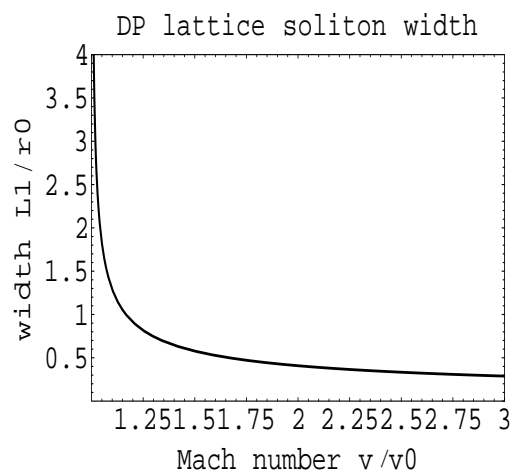


FIG. 9:

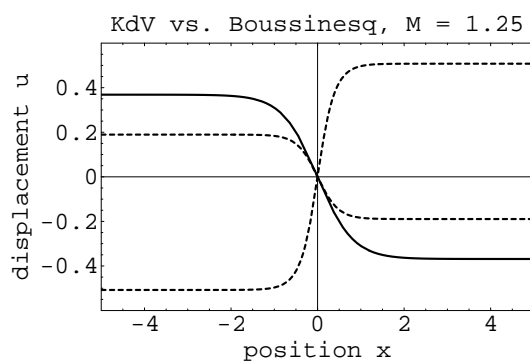
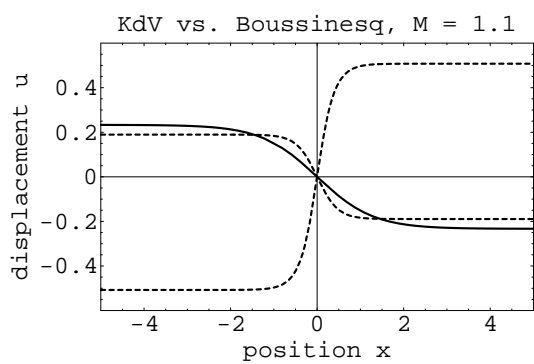
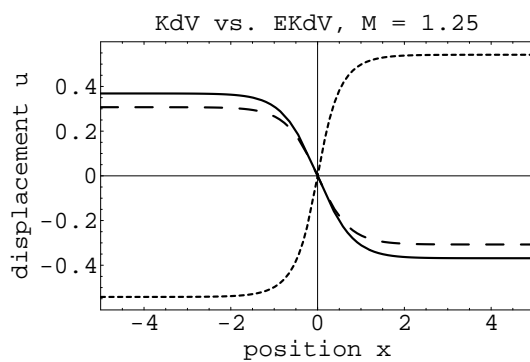
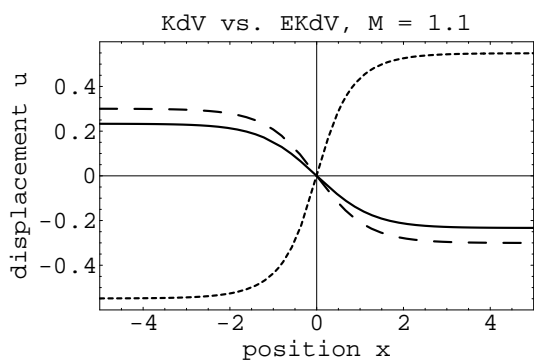


FIG. 10:

FIG. 11:

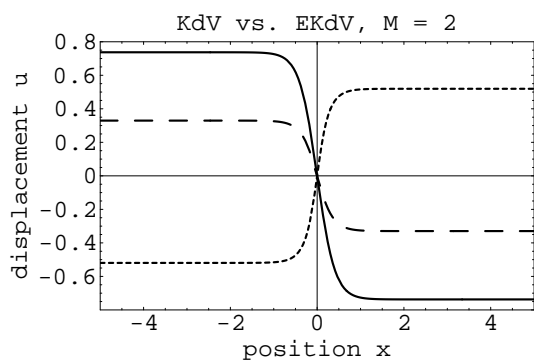


FIG. 12:

